Multiparameter quantum critical metrology

G. Di Fresco[1⋆], B. Spagnolo [1,2], D. Valenti[1] and A. Carollo [1,2]

1 Department of Physics and Chemistry "Emilio Segrè", Group of Interdisciplinary Theoretical Physics, Università di Palermo, Viale delle Scienze, Ed. 18, I-90128 Palermo, Italy.
2 Radiophysics Department, Lobachevsky State University, Nizhny Novgorod, Russia.
⋆ giovanni.difresco01@unipa.it

March 11, 2022

Abstract

Single parameter estimation is known to benefit from extreme sensitivity to parameter changes in quantum critical systems. However, the simultaneous estimation of multiple parameters is generally limited due to the incompatibility arising from the quantum nature of the underlying system. A key question is whether quantum criticality may also play a positive role in reducing the incompatibility in the simultaneous estimation of multiple parameters. We argue that this is generally the case and verify this prediction in paradigmatic quantum many-body systems close to first and second order phase transitions. The antiferromagnetic and ferromagnetic 1-D Ising chain with both transverse and longitudinal fields are analysed across different regimes and close to criticality.

1   Introduction

The main purpose of metrology is gaining the best accuracy possible in the estimation of physical parameters, both in classical [1] and quantum systems [2]. Quantum metrology exploits quantum effects to enhance the sensitivity in the estimation, providing advantages in a variety of applications which ranges from gravitational wave detection [3], measuring standards, magnetometry [4], thermometry, imaging [5,6], navigation, remote sensing, super-resolution [7–10] and many more [11]. Most of these applications intrinsically involve the estimation of multiple parameters at the same time, which explains the growing interest in multiparameter quantum metrology [12–14], both theoretically [15–42] and experimentally [43–47].

The extreme sensitivity to small parameter changes is one of the defining characteristic of quantum many-body systems near criticality [48,49]. The possibility of exploiting this sensitivity in single parameter metrology has attracted a growing interest in the last few years [50–59]. Therefore, a question naturally arises: can the advantages of using interacting many-body systems near criticality be extended to the simultaneous estimation of multiple parameters?

Answering this question is not straightforward, both on a conceptual and computational level. With respect to single parameter quantum metrology, the multiparameter case poses an extra challenge, arising from the very foundation of quantum mechanics: the incompatibility of multiple variables [60,61]. This results in a trade-off between uncertainties, which complicates in a non-trivial way the quest for the optimal simultaneous measurements already in finite dimensional systems [39,46,62]. Extending this problem to a many-body setup in presence of incompatibility is certainly a daunting task.

One way around this task is evaluating the extent to which this incompatibility affects the estimation problem. This can be done efficiently by resorting to a recently introduced quantity called *quantumness* [37,63]. The quantumness measures the *asymptotic incompatibility* of a multiparameter metrological problem in the limit of an infinite number of copies. The novelty and importance of this approach resides in its simplicity. Indeed, it allows the straightforward evaluation of the estimation's incompatibility from easy-to-compute quantities of the system of interest.

The standard bounds in the accuracy of a quantum multiparameter protocol are given in the form of a matrix inequality for the mean square error matrix by the quantum Cramer-Rao bound (QCRB) [2,64,65]. The QCRB is not always tight, due to the aforementioned incompatibility. Instead, the Holevo-Cramer-Rao bound (HCRB) stands out as the ultimate (scalar) bound of multiparameter quantum estimation problems [64], in that it is always achievable in collective measurements on asymptotically large number of copies [66–70]. However, the HCRB, except for few simple cases [71–74], is far from straightforward to compute, even numerically [39].

By contrast, the *quantumness*, denoted by R_λ[1], is a scalar quantity that can be easily evaluated through the quantum Fisher information matrix (QFIM) F_Q and the mean Uhlmann curvature (MUC) matrix U [75] and quantifies the discrepancy between the HCRB and the QCRB. Its values range in $R_\lambda \in [0,1]$, with $R_\lambda = 0$ if and only if the two bounds coincide, in which case the multiparameter estimation problem is *asymptotically compatible*. Its maximum value, $R_\lambda = 1$, marks the maximal discrepancy between the QCRB and the HCRB which in turn signals the maximal incompatibility between the parameters to be estimated, even in the asymptotic limit [76,77].

In this work, we analyze the compatibility of multiparameter quantum metrology near continuous quantum phase transitions (QPTs) and first order QPTs, using as a main figure of merit the quantumness along with the scaling properties of the QFIM. To this end, we consider

---

[1]The pedix λ denotes the set of parameters to be estimated in the metrological protocol

two paradigmatic models: a ferromagnetic and antiferromagnetic Ising chain, both interacting with transverse and longitudinal fields. Moreover, a third model, a spin-1/2 XY chain with transverse field, is also considered in appendix B.

Each multiparameter protocol displays peculiar features related to details of the model, however, when it comes to QPT, the quantumness tipically vanishes as criticality is approached. This can be understood using standard scaling arguments [48]. Close to a continuous phase transition physical quantities are characterised by power-law scalings in the system size L, hence one may assume that the quantumness scales as $R_\lambda \sim L^{d_R}$ where d_R is a suitable exponent. However, the upper bound $R_\lambda \leq 1$ [78] is only compatible with *non-positive exponents*, i.e. $d_R \leq 0$. Analogous arguments applied to first order phase transitions lead to similar conclusions, with scalings which are however dependent on the boundary conditions (Scaling analysis section). A further insight is also provided by the definition of the quantumness which reads [78]

$$R_\lambda = \left\| 2i F_Q^{-1} U \right\|_\infty, \tag{1}$$

where $\|X\|_\infty$ denotes the largest eigenvalue of X. The inverse dependence of R_λ on F_Q, which generally diverges at criticality, together with the fact that the MUC may at most diverge with the same rate as F_Q [78], explains the vanishing behaviour of R_λ. Hence, one may argue that the divergence of F_Q, which is the feature that makes critical systems highly attractive for single parameter quantum estimation, is also behind the mechanism responsible for the mitigation of the incompatibility.

2 Brief summary of the theoretical background

A system involved in a quantum estimation problem can be described by a family of quantum states ρ_λ labelled by a set of parameters λ, defined in a p-dimensional manifold M. A multi-parameter quantum estimation problem is a quest for the best accuracy possible in the simultaneous estimation of λ [42, 61, 63, 78]. The quantum Cramer-Rao bound (QCRB) provides a lower bound for the mean square errors of the parameters λ, which can be formally written as [42],

$$\Sigma \geq F_Q^{-1}, \tag{2}$$

where $\Sigma = \text{cov}(\hat{\lambda})$ is the covariance matrix of any locally unbiased estimators $\hat{\lambda}$ of the parameters λ and F_Q is the Fisher information matrix, whose components

$$F_{Q_{\mu\nu}} = \frac{1}{2} Tr \left(\rho_\lambda \{ L_\mu, L_\nu \} \right), \tag{3}$$

are defined in terms of $\{L_\mu\}_{\mu=1}^p$, a set of self adjoint operators known as *symmetric logarithmic derivatives* (SLD), each satisfying the equation

$$\frac{L_\mu \rho_\lambda + \rho_\lambda L_\mu}{2} = \partial_\mu \rho_\lambda, \tag{4}$$

where $\partial_\mu = \partial / \partial_{\lambda_\mu}$. As mentioned in the introduction, the bound in Eq. (2) is not always tight, unless the following compatibility condition is met [42, 61]

$$U_{\mu\nu} = -\frac{1}{4} \text{Tr} \left\{ \rho_\lambda \left[L_\mu, L_\nu \right] \right\} = 0 \quad \forall \mu, \nu, \tag{5}$$

where $U_{\mu\nu}$ is known as *mean Uhlmann curvature* [63, 75], a quantity which reduces to the Berry curvature when ρ_λ is a family of pure states. The compatibility condition (5) ensures that the

discrepancy between the QCRB and the Holevo-Cramer-Rao bound (HCRB) is zero [42]. The discrepancy between the two bounds can be expressed as

$$D(W) = \text{tr}\left(W\Sigma F_Q^{-1}\right) - C_H(W), \tag{6}$$

where W is a positive definite weight matrix and $C_H(W)$ is the HCRB [42]

$$\begin{aligned}
\text{tr}\left[W\Sigma\right] &\geq \min_{\{X_i\}}\Big\{\text{tr}\left[W\Re(V)\right] \\
&+ \left\|\sqrt{W}\Im(V)\sqrt{W}\right\|_1\Big\} = C_H(W),
\end{aligned} \tag{7}$$

with $\|\cdot\|_1$ being the operator trace norm ($\|\cdot\| = \text{tr}(|\cdot|)$), $V_{i,j} = \text{tr}\left(X_i X_j \rho_\theta\right)$, and the minimization being performed over the Hermitian matrices X_i, satisfying $\frac{1}{2}\text{tr}\left(\{X_i, L_j\}\rho_\theta\right) = \delta_{i,j}$. This last constraint plays the role of the local unbiasedness condition. It should be pointed out that the minimization performed in Eq. (7) makes really difficult to evaluate the HCRB for systems of interest. The discrepancy in Eq. (6) satisfies [78]

$$0 \leq D(W) \leq \text{tr}\left(W F_Q^{-1}\right) R_\lambda, \tag{8}$$

where R_λ is a scalar index, known as *quantumness*, defined as

$$R_\lambda = \left\|2i F_Q^{-1} U\right\|_\infty, \tag{9}$$

with $\|X\|_\infty$ denoting the largest eigenvalue of X, and the pedix λ specifying the set of parameters to be estimated in the metrological protocol. As already noted, the value of R_λ ranges in $[0,1]$: the limit $R_\lambda = 0$ is equivalent to Eq. (5), and therefore denotes compatibility, whereas $R_\lambda = 1$ marks the maximal incompatibility of the metrological problem. The quantumness obeys a monotonic behaviour with respect to quantum estimation sub-model [76] that could be formalized as follows. If $R_\lambda^{(p)}$ is the quantumness of an estimation model defined by a set of p parameters $\boldsymbol{\lambda}$, and $R_{\tilde{\boldsymbol{\lambda}}}^{(p-1)}$ is the quantumness of the possible sub-model defined by a subset of (possibly reparameterised) $p-1$ parameters $\tilde{\boldsymbol{\lambda}}$, they satisfy the following bound

$$R_{\tilde{\boldsymbol{\lambda}}}^{(p-1)} \leq R_\lambda^{(p)}. \tag{10}$$

In other words, any multi-parameter estimation protocol is incompatible at least as much as any of its sub-models. This also means that evaluating the quantumness of a full multi-parameter estimation protocol may hide possible compatibilities between some of its parameters. In this sense, it may be more informative to analyse the quantumness of some of its sub-models separately.

In particular, for a two-parameter estimation problem the expression for the quantumness acquires a particularly simple form [37]

$$R_\lambda^{(2)} = \sqrt{\frac{\det(2U)}{\det(F)}}. \tag{11}$$

3 Scaling analysis

In this section we provide a scaling analysis of the quantumness close to QCP. This analysis shows that R_λ cannot increase close to QCP and generally decreases with a critical exponent which depends both on the property of the critical system and on the chosen parameters. We follow closely the method reported in Ref. [79, 80] that can be applied to study the finite size scaling (FSS) of both continuous and first order quantum phase transition (QPT). We first focus on a continuous QPT.

3.1 Continuous phase transition

Let us suppose to have a d-dimensional lattice model with linear size L, whose Hamiltonian $H(\boldsymbol{\lambda})$ depends on the set of parameters $\{\lambda_\mu\}$. The critical point of a continuous QPT is characterized by scale invariance, and by power-law behaviours of physical quantities which have universal character. Such a universal behaviour emerges between microscopic Hamiltonians which differ by terms, known as irrelevant operators, that become vanishingly small under coarse-graining transformation of the lattice. In such a situation, one can extract information on the universal properties of the system by performing scaling transformations that modify the lattice spacing $a \to \alpha a$. As a consequence, lengths and time rescale as $x \to x\alpha$ and $t \to t\alpha^z$ [48], where z is the dynamical critical exponent. Around the critical point, each local operator can be decomposed in a set of operators, called relevant operators, which dominates the physical property of the system and obey a power-law scaling, $\mathcal{O}_i \to \alpha^{-d_i}\mathcal{O}_i$, where d_i is the operator scaling dimension. If one of the parameter, e.g. λ_μ, drives the system close to the criticality, the correlation length of the system is given by $\xi_\mu = (|\lambda_\mu - \lambda_\mu^c|/\lambda_\mu^c)^{-\nu_\mu}$, where λ_μ^c is the critical value of the parameter and ν_μ is the correlation length critical exponent.

One can use the scaling behaviours with respect to α in conditions in which the system nearly obeys scale invariance. The most relevant perturbation which breaks the scale invariance dominates the scaling behaviour. For example, if $L \gg \xi_\mu$, the most relevant perturbation is given by $\alpha \sim \xi_\mu^{-1} = (|\lambda_\mu - \lambda_\mu^c|/\lambda_\mu^c)^{\nu_\mu}$. On the other hand, close to criticality in a finite system with size $L \ll \xi_\mu$, the system is dominated by system size effect and $\alpha \sim L^{-1}$ is the most relevant perturbation. The latter is the regime on which we focus.

As for any other physical quantity, one may assume that the quantumness obeys a scaling law $R_\lambda \sim \alpha^{-d_R}$, which in a finite size regime, with $L \ll \xi_\mu$, implies that

$$R_\lambda \sim L^{d_R}. \tag{12}$$

As mentioned in the introduction, the upper bound $R_\lambda \leq 1$ [78], is only compatible with a *non-positive exponent*, i.e. $d_R \leq 0$.

Although, this argument is quite general, one can make a more detailed analysis on the scaling behaviour of the quantumness, based on the scaling properties of F_Q and U and on the universal properties of the underlying model. To this end, we will assume that the operators $\partial_\mu H$ can be expressed as the sum of local operators i.e. $\partial_\mu H = O_\mu = \sum_x O_\mu(x)$, where x labels a spatial position on the lattice, and that O_μ's are relevant operators with scaling dimension d_μ's. For the system in its ground state, $F_{Q\mu\nu}$ and $U_{\mu\nu}$ can be expressed in a compact form [78, 81, 82]

$$F_{Q\mu\nu} = \frac{2}{\pi} \int_{-\infty}^{+\infty} \frac{d\omega}{\omega^2} \mathcal{S}_{\mu\nu}^+(\omega) \tag{13}$$

$$U_{\mu\nu} = \frac{i}{\pi} \int_{-\infty}^{+\infty} \frac{d\omega}{\omega^2} \mathcal{S}_{\mu\nu}^-(\omega) \tag{14}$$

where $\mathcal{S}_{\mu\nu}^\pm(\omega) := \frac{\mathcal{S}_{\mu\nu}(\omega) \pm \mathcal{S}_{\nu\mu}(\omega)}{2}$ are the symmetric and anti-symmetric parts of the dynamical structure factor $\mathcal{S}_{\mu\nu}(\omega) := \int_{-\infty}^{\infty} dt\, e^{i\omega t} \langle O_\mu(t) O_\nu \rangle$, and $O_\mu(t) := e^{iHt} O_\mu e^{-iHt}$.

The scaling of F_Q close to a critical point can be derived from the symmetric structure factors, which scale as $\int_{-\infty}^{\infty} d\omega \mathcal{S}_{\mu\nu}^+ \sim \langle \{O_\mu, O_\nu\} \rangle \sim \alpha^{-d_\mu - d_\nu}$, and $\omega \to \omega\alpha^{-z}$. Thus, from Eqs. (13) we get

$$F_{Q\mu\nu} \to F_{Q\mu\nu} \alpha^{-d_\mu - d_\nu + 2z}. \tag{15}$$

On the other hand, the anti-symmetric structure factor scales as $\int_{-\infty}^{\infty} d\omega \mathcal{S}_{\mu\nu}^- \sim \langle [O_\mu, O_\nu] \rangle$, with a dependence on the commutator which scales with an exponent $d_{\mu\nu}^- \leq d_\mu + d_\nu$. Accordingly,

from Eq. (14) we obtain the following scaling for $U_{\mu\nu}$

$$U_{\mu\nu} \to U_{\mu\nu}\alpha^{-d_{\mu\nu}^- + 2z}. \tag{16}$$

According to Eq. (9) or its two parameter version (Eq. (11)), and in the hypothesis in which the scaling of F_Q and U is dominated by their universal behaviours, we obtain

$$R_\lambda \to R_\lambda \alpha^{-d_R} \qquad \text{with} \quad d_R = d_{\mu\nu}^- - d_\mu - d_\nu \leq 0. \tag{17}$$

For a system with finite size at the critical point the scale invariance is broken by the system size, which scales as $L \sim \alpha^{-1}$, yielding

$$R_\lambda \sim L^{d_R} \quad \text{with} \quad d_R < 0. \tag{18}$$

Alternatively, by exploiting the relation (34), one can compute the scaling of F_Q from the that of the fidelity, as

$$\mathcal{F}(\lambda, \delta\lambda, L) = 1 - \tfrac{1}{8}\sum_{\mu,\nu}\delta\lambda_\mu\delta\lambda_\nu F_{Q_{\mu\nu}} + 0\left(\delta\lambda^3\right), \tag{19}$$

where $\mathcal{F}(\lambda, \delta\lambda, L)$ denotes the fidelity between infinitely close ground states $\psi(\lambda)$ and $\psi(\lambda+\delta\lambda)$ of a system of size L^d. By following standard scaling argument [48] any physical observable $\mathcal{O}$ close to a QCP can be expressed in terms of a scaling function $f_{\mathcal{O}}(\kappa)$ as

$$\mathcal{O} \approx L^{-y_{\mathcal{O}}} f_{\mathcal{O}}(\kappa) \tag{20}$$

where $y_{\mathcal{O}}$ is the scaling dimension of $\mathcal{O}$ and $\kappa = \{\kappa_\mu\}$ is a collection of suitable combinations of parameters λ and L as

$$\kappa_\mu = \lambda_\mu L^{y_\mu} \tag{21}$$

Generalising the arguments in Ref. [79] to multiparameter scenarios we can express the fidelity close to QPT in terms of the rescaled parameterisation as

$$\mathcal{F}(\lambda, \delta\lambda, L) \approx \mathcal{F}(\kappa, \delta\kappa), \tag{22}$$

where the dependence on L is implicit in κ, and $\delta\kappa$ are variations due to $\delta\lambda$. Now expanding $\mathcal{F}$ in power of $\delta\kappa$ as

$$\mathcal{F}(\kappa, \delta\kappa) = 1 - \sum_{\mu,\nu}\delta\kappa_\mu\delta\kappa_\nu f_{\mu\nu}(\kappa) + o\left(\delta\kappa^3\right) \tag{23}$$

and combining Eq.(19) and Eq.(23), it is possible to obtain the QFIM as

$$F_{Q_{\mu\nu}} \approx 8L^{y_\mu + y_\nu} f_{\mu\nu}(\kappa). \tag{24}$$

Again, the scaling of the quantumness for a two parameter model can be inferred from Eq. (11) and from the scaling of F_Q and U. As argued already, the scaling of the determinant of MUC is always bounded above by the scaling of the determinant of QFIM. This can be deduced from Schrödinger-Robertson uncertainty inequality applied to the SLD [83]

$$\det\left[\frac{1}{2}\mathrm{Tr}\rho\{L_\mu, L_\nu\}\right] \geq \det\left[-\frac{i}{2}\mathrm{Tr}\rho[L_\mu, L_\nu]\right], \tag{25}$$

which, compared to Eqs. (3) and (5), yields

$$\det F_Q \geq \det 2U. \tag{26}$$

If, for simplicity, we assume F_Q in diagonal form, then $\det F_Q \approx L^{2(y_\mu + y_\nu)}f_{\mu\mu}f_{\nu\nu}$, and $\det U \approx L^{2u}f_u$ with $u \leq y_\lambda + y_\sigma$. And we find again the scaling of the quantumness as

$$R_{\lambda\sigma} \approx L^{u-(y_\lambda + y_\sigma)}f_R = L^{y_R}f_R, \tag{27}$$

where $y_R \leq 0$.

3.2   First order phase transition

It is possible to apply a similar procedure to study first order QPT scaling. The scaling behavior of this kind of QPT is crucially dependent on the boundary conditions [79]. As before, let us assume to have an Hamiltonian $H(\boldsymbol{\lambda})$ dependent of a set of parameters $\boldsymbol{\lambda} = \{\lambda_\mu\}$ and let's study the FSS in proximity of a first order QPT. First order QPT generally arises from level crossing, which only occurs in the infinity-volume limit. For finite size systems, the QPT is characterised instead by avoiding level crossings, whose energy gap rules the FSS behaviour. Following Ref [80] we define the avoiding level crossing energy gap

$$\Delta_0(L) = \Delta(\boldsymbol{\lambda} = \boldsymbol{\lambda}^c, L), \tag{28}$$

where $\boldsymbol{\lambda}^c$ are critical values of the parameters, and we introduce a set of rescaled parameters which characterize the FSS

$$\tilde{\lambda}_\mu = \frac{E_\mu(\boldsymbol{\lambda}, L)}{\Delta_0}, \tag{29}$$

where $E_\mu(\boldsymbol{\lambda}, L)$ is the energy gap variation due to a change in λ_μ from its critical value λ_μ^c. By following a similar argument as in [79] one can derive the following scaling

$$F_{Q\mu,\nu} \sim \frac{(\partial_\mu E_\mu)(\partial_\nu E_\nu)}{\Delta_0^2(L)}. \tag{30}$$

Notice that the divergence of the QFIM with sistem size is strongly influenced by the dependence of the energy gap $\Delta_0(L)$. Depending on the type of boundary condition, the gap may vanishes exponentially with the system size, i.e. $\Delta_0(L) \sim e^{-aL^d}$ or with a power-law behaviour, $\Delta_0(L) \sim L^{-b}$ [80]. In either case, using the same argument as in the previous section, one can show that the scaling of U is bounded by that of F_Q, and the quantumness must scale as

$$R \sim \frac{y_U \Delta_0^2(L)}{(\partial_\mu E_\mu)(\partial_\nu E_\nu)} \leq 1. \tag{31}$$

Notice the dependence of $\Delta_0(L)$ in Eq. (31), which is compatible with an exponential or power-law scaling to zero, depending on the boundary conditions.

4   Ising model with transverse and longitudinal fields.

We analyse the metrological properties of a 1-D quantum Ising chain with a transverse magnetic field in x and y directions, and a longitudinal magnetic field in z direction. The parameters to be estimated are the coupling constants of the magnetic field, appearing in the Hamiltonian

$$H = -\sum_{i=1}^{n} \sigma_i^z \sigma_{i+1}^z + h_x \sigma_i^x + h_y \sigma_i^y + h_z \sigma_i^z, \tag{32}$$

where σ_i are the Pauli matrices and n is the number of spins. This kind of estimation protocol cannot be interpreted as a canonical interferometric metrological scheme [84]. Rather, this coincides with the standard picture used in single-parameter quantum critical metrology, whereby the Hamiltonian parameters are estimated through the effects they have on corresponding equilibrium state [50, 51, 54, 58]. Therefore, we can find an estimate of the parameters of interest by studying how the properties of the probe states change as the Hamiltonian parameters varies. To analyse in details the compatibility of this model we will consider the quantumness associated to pairs of magnetic field amplitude, which we will denote $R_{\mu\nu} \equiv R_{\{h_\mu, h_\nu\}}$ with $\mu, \nu \in \{x, y, z\}$.
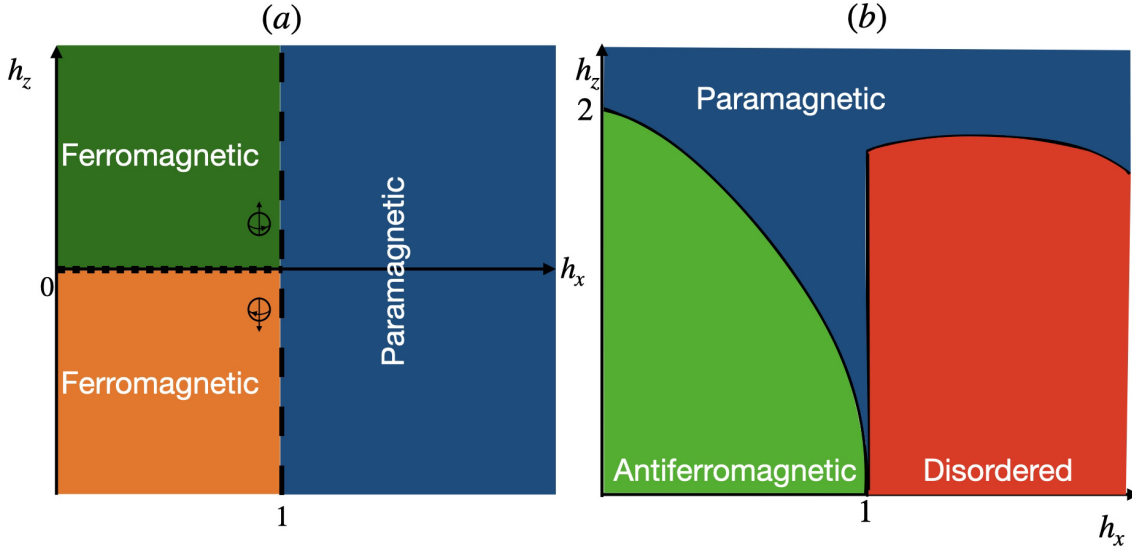
Figure 1: Panel (a): phase diagram of the ferromagnetic 1-D Ising chain with longitudinal and transverse magnetic fields. Panel (b): phase diagram of the antiferromagnetic 1-D Ising chain with longitudinal and transverse magnetic fields.

At $h_z = 0$, $h_y = 0$ $(h_x = 0)$ and $h_x = 1$ $(h_y = 1)$ the model undergoes a continuous QPT belonging to the two-dimensional Ising universality class, separating a disordered phase $(h_x > 1)$ from an ordered one $(h_x < 1)$. For any point in $|h_x - h_y| < 1$, the longitudinal field drives a first order QPT along the $h_z = 0$ plane (see panel (a) of Fig. 1). We will limit to study the system at $T = 0$, hence we can choose the ground state of Eq. (32) as input probe, which on the one hand allows capturing the features of the QPT, and on the other simplifies the evaluation of QFIM and MUC. Note that the presence of a longitudinal field term in Eq. (32) breaks the integrability of the Hamiltonian and the estimation problem requires a numerical approach. Despite the further complication due to the non-analyticity of the problem, the presence of a longitudinal term h_z allows us to add in the estimation problem a parameter that couples with the order parameter of the second order QPT $(\langle S_z \rangle)$. This provides the opportunity to test the role of the order parameter in the estimation problem.

The Hamiltonian in Eq. (32) is numerically diagonalized through the application of the *implicitly restarted Lanczos method*. Due to the lacking of an analytic expression for the ground state of Eq. (32), we will resort to the fidelity approach to calculate the QFIM susceptibility (See appendix A). This approach is a multiparameter generalization of the method used in Ref. [79, 85]. After computing the ground states for two relatively close values of the parameters, the fidelity can be calculated as the overlap between these two states. This procedure is repeated with different pairs of states which are taken progressively away from each other along the λ_i direction on the parameter space. Eventually, the fidelity susceptibility is found through a parabolic fitting of the fidelity against λ_i [79]. Similarly, the MUC can be evaluated with a numerical approach similar to that of Ref. [86]. Exploiting the relation with the Berry curvature for pure states, the MUC can be computed through the Bargmann phase [87, 88], which is a version of the Berry phase evaluated on a discretized circuit in the parameter space (see appendix A). The results of these calculations are used to evaluate R_λ through its analytic expression (9), across the phase diagram, as displayed in panel (a) of Fig. 2.

A detailed numerical analysis of the quantumness displays an apparent insensitivity across the QPT in $(h_x = 1, h_y = 0, h_z = 0)$. Specifically, we find that for $h_y = h_z = 0$ and $h_x \in (0, 2]$ the quantumness is constantly equal to $R_{xy} = R_{xz} = 0$ and $R_{yz} = 1$.

This trivial behaviour, not shown here, of the quantumness is due to the overwhelming
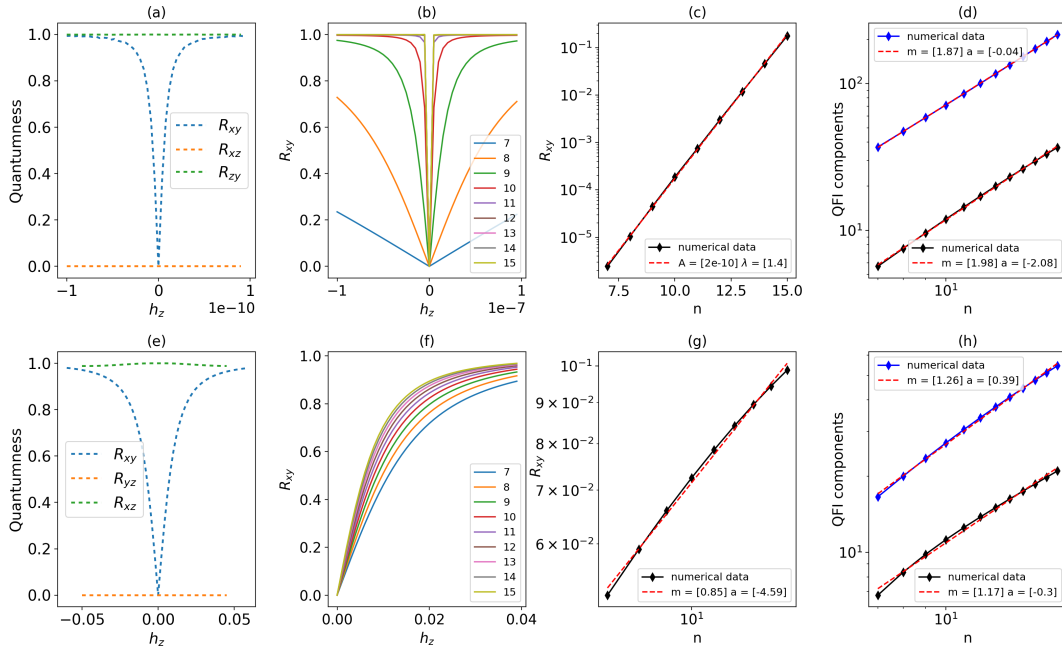
Figure 2: In panel (a) and (e) is shown the behaviour of the quantumness for each pair of magnetic fields respectively for $h_x = 0.2$ and $h_x = 1.2$ and with $n = 11$ as a function of h_z. In panel (b) is shown the scaling behaviour of the quantumness for $h_x = 0.3$ as a function of h_z. In the semi-log plot in panel (c) that reports the quantumness as a function of n is shown that, in the presence of the first order QPT ($h_x = 0.3$), the quantmuness has an exponential scaling with respect to the number of spins n. Panels (f) and (g) (log-log plot), that displays R_{xy} as a function respectively of h_z and n, show the scaling behaviour in absence of the first order QPT for $h_x = 1.2$, highlighting a power-law scaling of R. In the log-log plots in panel (d) and (h) is shown the scaling behaviour of the x (in black) and y (in blue) components of the QFI with respect to the number of spins n. In panel (d) it is shown that for $h_x = 0.95$ both the components reach a Heisenberg scaling. Otherwise, in panel (h) in absence of QPT ($h_x = 1.2$) both components have a normal quantum scaling. Notice that the fitting parameters m and a are respectively the slope and the intercept of the linear fitting, while A and λ are the amplitude and the coefficient of the exponential fitting, respectively.

effects of the first order phase transition, which hides the dependence of $R_{\mu\nu}$ on the continuous QPT.

On the other hand, panel (a) and (e) of Fig. 2 displays the behaviour of $\left(R_{xy}, R_{xz}, R_{yz}\right)$ versus the longitudinal field h_z, for $h_y = 0$ and h_x fixed. Also in this case R_{xz} and R_{yz} are insensitive to the field, both in the ordered phase (panel (a), $h_x = 0.2$) and in the disordered one (panel (e), $h_x = 1.2$). Panel (a) shows that the only component sensitive to the first order QPT is R_{xy}, with a sharp reduction to zero across $h_z = 0$, for $h_x < 1$ (ordered phase). However, panel (e) of Fig. 2 shows that R_{xy} goes to zero also for $h_x > 1$ (region in which no first order phase transition is present). Despite the apparent similarity in the behaviours of R_{xy} for $h_x > 1$ and $h_x < 1$, their behaviour is qualitatively different in the two regions, due to the presence (in the ordered phase) and absence (in the disordered phase) of a first order QPT. In order to show that R_{xy} is actually sensitive to the first order QPT, we report in panels (b) and (f) of Fig. 2 the scaling behaviour with the system size of R_{xy} in the two different regions.

In panel (b), when the system crosses $h_z = 0$ with $h_x < 1$, the first order QPT occurs and

R_{xy} goes abruptly to zero with a rate which grows exponentially with the number of spins, as shown explicitly in panel (c). On the contrary, panel (f) displays the behaviour of R_{xy} across $h_z = 0$, in the disordered region ($h_x > 1$), where no first order QPT occurs: here the quantumness goes smoothly to zero with a rate which is power-law dependent on the system size (see also panel (g) for a power-law fitting).

From a metrological point of view it is also meaningful to study closely the behaviour of the QFI and its scaling near the phase transition. Panels (d) and (h) in Fig. 2 show that the QFI has different scaling behaviours in the two regions of the phase diagram. In panel (d) it is shown that in the ferromagnetic region, with h_x near 1, both the x and y components of the QFI have a Heisenberg-like scaling that allows to perform precise estimation in each direction. Otherwise, in the paramagnetic region (panel (h)) both the components of the QFI have a normal quantum scaling.

The behaviour of the two components of the inverse QFI is not far from that of the reciprocal QFI since, despite their presence, the off-diagonal elements in the QFI matrix are order of magnitude smaller than the diagonal elements.

5 Antiferromagnetic Ising chain.

Due to the presence of a longitudinal magnetic field, the antiferromagnetic Ising chain has different properties from those of the ferromagnetic one. In fact, the Hamiltonian

$$H = \sum_i \sigma_i^z \sigma_{i+1}^z - h_x \sigma_i^x - h_y \sigma_i^y - h_z \sigma_i^z \tag{33}$$

is characterized by a completely different phase diagram, as we can see from panel (b) of Fig. 1 [89]. The main difference, in the region of interest, lies in a stable antiferromagnetic phase for values of the longitudinal magnetic field different from zero with a consequent line of continuous QPTs in which $h_z \neq 0$. This shifts our focus in a region of the parameter space in which more than one component of the magnetic field is non vanishing.

To map the Hamiltonian in Eq. (33) into a ferromagnetic model we need a staggered magnetic field [90], which justifies the differences between the models. We notice that the phase diagram in panel (b) of Fig. 9 can be derived through the fidelity approach [89]. In Ref. [89] it is shown that at the phase transition from an antiferromagnetic to a paramagnetic order, the x component of the QFI matrix exhibits a maximum. Here we study closely the scaling behaviour of the QFI at the transition point and how it affects the compatibility index. We also use only even numbers of spins, to avoid frustration due to the antiferromagnetic nature of the chain, and periodic boundary conditions. As for the ferromagnetic scenario, R_{xy} is, again, the only component of the quantumness sensitive to the phase transition. However, the different properties of the model affects profoundly the behaviour of the quantumness, leading to a completely different behaviour. Fig. 3 shows that $R_{xy} < 1$ in all the range of the parameters evaluated and that at the phase transition the critical behaviour of the QFI makes the quantumness vanish as the size of the chain increases. In panel (a) of Fig.4 it is reported the scaling behaviour of the QFI for $h_x = 0.5$: the x component exhibits a maximum and it reaches a Heisenberg scaling (QFI$\sim N^2$), whereas the y component at the critical point has a standard quantum scaling (QFI$\sim N$). So, at criticality, the system reaches the highest precision in one of the two components while displaying asymptotic compatibility with the other component. Panel (b) of Fig. 4 shows the dependence on system size of the determinants of QFI and MUC, which both display a power-law scaling. Since the QFI has a scaling higher than the MUC, from Eq. (9) we can extrapolate that the quantumness asymptotically vanishes at the criticality.
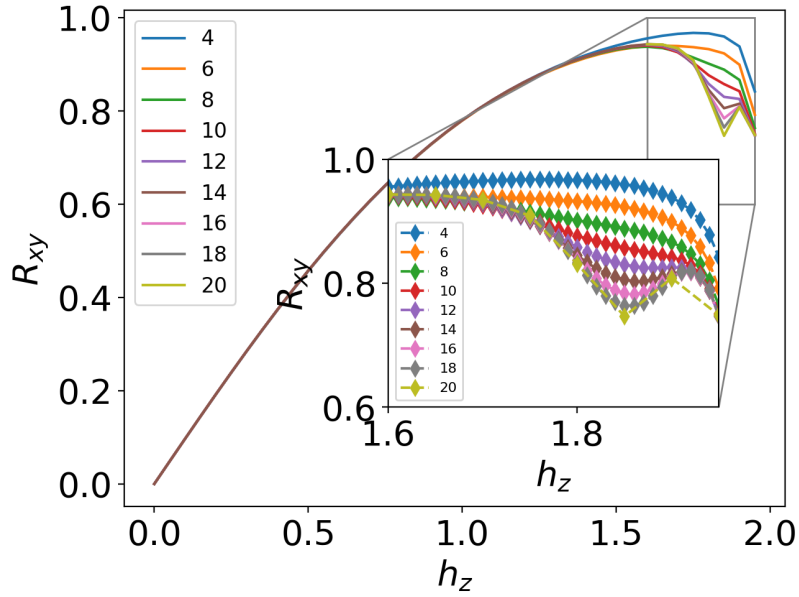
Figure 3: The compatibility index R_{xy} for different values of the chain size and $h_x = 0.2$ as a function of the longitudinal field h_z. The inset shows the behaviour of the compatibility index near the critical point.
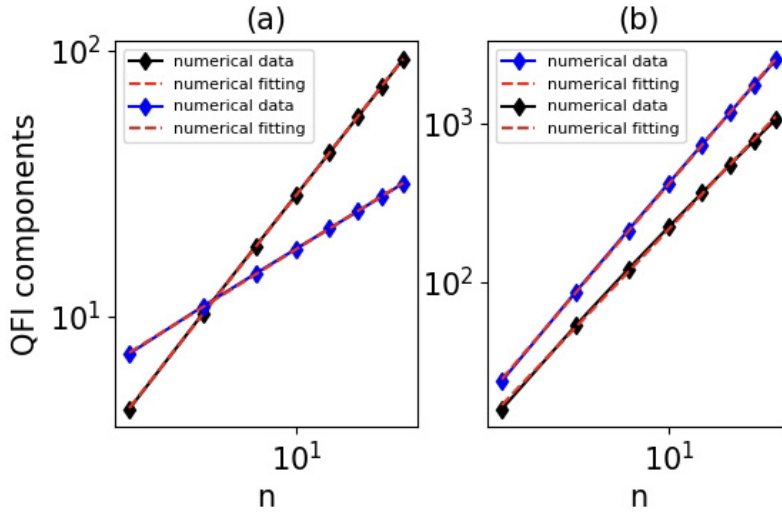
Figure 4: In panel (a) The log-log plot of the diagonal components of the quantum Fisher information whit $h_x = 0.5$ at the critical point. In blue the scaling of the y component, with a slope $m = 0.98$ and an intercept $a = 0.63$, and in black that of the x component, with a slope $m = 2.01$ and an intercept $a = -1.28$, as a function of the number of spins n. In the log-log plot in panel (b) it is reported in blue the scaling behaviour of the quantum Fisher information matrix determinant at the critical point for $h_x = 0.5$ as a function of the number of spins n, with a slope $m = 3.09$ and an intercept $a = -1.086$. In black it is reported the scaling behaviour of twice the mean Uhlmann curvature determinant at the critical point for $h_x = 0.5$, with a slope $m = 2.784$ and an intercept $a = -1.037$

6 Conclusion

In this work we have analyzed the performance of multiparameter quantum critical estimation protocols focusing on the role of QPT in mitiganting the incompatibility among parameters. From the prototypical models analyzed, in both first and second order QPT, a common feature emerging is the strong dependence of R_λ on criticality, and a general influence of QPT in reducing the incompatibility. In a two-parameter magnetometry model with a 1D Ising chain, the sensitivity of the quantumness to a first order QPT is numerically demonstrated. Indeed, the exponential scaling of R_λ represents a signature of the first order QPT. A similar setup, in an antiferromagnetic scenario, displays an asymptotic compatibility at the critical point, demonstrated by a vanishing behaviour of R_λ.

Our work strongly suggests that quantum critical metrology provides a promising framework for multi-parameter estimation. One of the desirable features of critical metrology, i.e. the divergence of the Fisher information, comes with an extra advantage in the multi-parameter scenario: criticality may help in mitigating the incompatibility. The latter is one of the main drawback in quantum multi-parameter metrology, which makes the estimation challenging both on a computational and a conceptual level. Our approach opens up the possibility to explore multi-parameter metrology in many-body setups using easy-to-compute figures of merit, thereby paving the way to fundamental theoretical advances and technological applications.

Acknowledgements

This work was supported by Italian Ministry of University and Research (MUR) and the Government of the Russian Federation through Agreement No. 074-02-2018-330 (2).

Author contributions **GDF:** Conceptualization; Data curation; Formal analysis; Investigation; Methodology; Software; Validation; Visualization; Roles/Writing - original draft; Writing - review & editing.
BS: Conceptualization; Formal analysis; Funding acquisition; Investigation; Methodology; Writing - review & editing.
DV: Conceptualization; Formal analysis; Funding acquisition; Investigation; Methodology; Writing - review & editing.
AC: Conceptualization; Data curation; Formal analysis; Funding acquisition; Investigation; Methodology; Software; Validation; Roles/Writing - original draft; Writing - review & editing.

A Numerical procedure

In the case of non-integrable system, the lacking of closed form expressions for the ground states prevents the calculation of the QFIM and MUC through the SLD. Instead, one can evaluate the QFIM through the fidelity susceptibility, by exploiting the following relation [65, 78, 85]

$$F_{Q\mu\nu} = -4\partial_\mu\partial_\nu\mathcal{F}[\rho_\lambda, \rho_{\lambda+\delta}], \tag{34}$$

where δ is a small variation of the parameters along the directions λ_μ and λ_ν, and $\mathcal{F}[\rho, \sigma] = \mathrm{Tr}\left(\sqrt{\sqrt{\rho}\,\sigma\sqrt{\rho}}\right)$ is the quantum Uhlmann fidelity [91] beetween ρ and σ, which for pure states reduces to the state overlap $\mathcal{F}[\psi, \psi'] = |\langle\psi|\psi'\rangle|$.
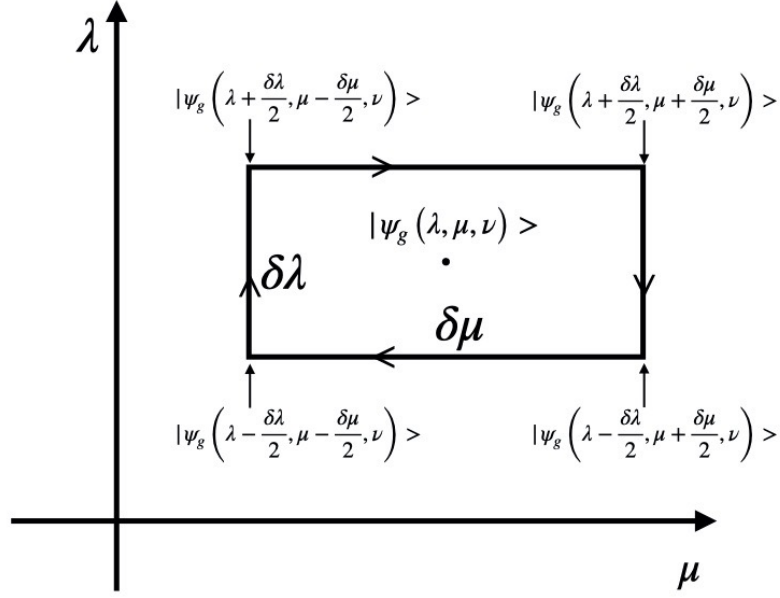
Figure 5: Rectangular circuit in the parameter space.

Similarly, when only pure states are involved, the MUC coincides with the Berry curvature [78], i.e.

$$U_{\mu\nu} = i\langle\partial_\mu\psi|\partial_\nu\psi\rangle - i\langle\partial_\nu\psi|\partial_\mu\psi\rangle. \tag{35}$$

In turns the Berry curvature can be thought of as the geometric phase per unit area on an infinitesimal loop on the parameter spaces [78], and it can be evaluated with numerical methods specifically designed for geometric phases [86]. This numerical methods consists in the evaluation of a discretised version of the Berry phase, namely the Bargmann phase [86–88], which is defined as

$$\Phi = \arg\{\prod_{i=0}^{N-1}\langle\psi_i|\psi_{i+1}\rangle\}. \tag{36}$$

where $\{\psi_i\}_{i=0}^{N-1}$ (with $\psi_N = \psi_0$) is a set of states lying on the vertices of a discrete close loop on the parameter space. The calculation of the MUC in a given point λ of the parameter space is obtained via the Bargmann phase per unit area evaluated on an infinitesimal loop, i.e.

$$U_{\mu\nu}(\lambda) = \lim_{\delta A\to 0}\frac{\Phi_{\mu\nu}(\lambda)}{\delta A}, \tag{37}$$

where $U_{\mu\nu}(\lambda)$ is the matrix element of the MUC, $\Phi_{\mu\nu}(\lambda)$ is the Bargmann phase calculated on an infinitesimal loop centred on λ and lying on the plane identified by the parameters λ_μ and λ_ν, and δA is the area of the loop. An example is shown in Fig. 5, where the states picked for the computation are on the vertices of the infinitesimal rectangle of sides $\delta\lambda_\mu$ and $\delta\lambda_\nu$. Moreover, to improve the numerically stability of the value of $U_{\mu\nu}$, we exploit the linear dependence of $\Phi_{\mu\nu}(\lambda)$ on δA and evaluate $U_{\mu\nu}$ through a linear fitting of $\Phi_{\mu\nu}(\lambda)$ against δA.

B   Ground state rotation of the XY spin chain.

We report here on a model that, unlike the two discussed in the previous sections, can be interpreted as a canonical interferometric model, in which the parameters to be estimated are

introduced through a unitary operator. We show that even in this scenario the quantmuness is strongly affected by criticality. The model analyzed is a XY spin chain, whose Hamiltonian is

$$H = -\sum_{i=-M}^{M} \left(\frac{(1+\gamma)}{2} \sigma_i^x \sigma_{i+1}^x + \frac{(1-\gamma)}{2} \sigma_i^y \sigma_{i+1}^y + \lambda \sigma_i^z \right), \tag{38}$$

where the sigmas are the Pauli matrices, γ is the anisotropic parameter, and λ is the strength of the external field. We limit our analysis to a region of the phase diagram with $\gamma \in (0,1]$, in which the criticality is at $\lambda_c = 1$ and belongs to the Ising universality class [49,92]. Moreover, we only consider the case $T = 0$, in order to capture the essential behaviour of quantum phase transitions. Finally, we assume that the input probe of the estimation is

$$\rho_0 = |\psi_g\rangle\langle\psi_g|, \tag{39}$$

where $|\psi_g\rangle$ is the ground state of Eq. (38). The set of parameters to be estimated is $\varphi = \{\varphi_x, \varphi_y, \varphi_z\}$ with

$$\rho_\varphi = U_\varphi^\dagger \rho_0 U_\varphi \quad \text{and} \quad U_\varphi = e^{i\left(\varphi_x S_x + \varphi_y S_y + \varphi_z S_z\right)}, \tag{40}$$

where φ_μ with $\mu = \{x, y, x\}$ are the angles by which the probe state is rotated and $S_\mu = \sum_i \sigma_i^\mu/2$ are the corresponding global spin operators. This unitary transformation can be thought of as the result of adiabatic variation of the parameter φ in the system Hamiltonian $U_\varphi^\dagger H U_\varphi$. This coincides whit the standard picture used in single-parameter quantum critical metrology, whereby the Hamiltonian parameters are estimated through the effects they have on the corresponding equilibrium state [50, 51, 54, 58]. Alternatively, this unitary transformation can be the result of a dynamical evolution applied to the initial probe state ρ_0. In this sense the protocol bears close similarity with the standard interferometric paradigm of quantum metrology [84]. We exploit the unitary symmetry of the problem, thus confining ourselves to the estimation around the point where $\varphi_x = \varphi_y = \varphi_z = 0$. For a pure state probe the SLD [61] is easily calculated, yielding in our case

$$L_\mu = 2\partial_{\varphi_\mu}\rho = 2i\left[S_\mu, \rho\right] \quad \mu = \{x, y, z\}, \tag{41}$$

which in turn leads to the following expressions for the matrix elements of QFIM and MUC

$$F_{\mu\nu} = 4C\left(S_\mu, S_\nu\right), \tag{42}$$

$$U_{\mu,\nu} = -i\text{Tr}\left(\rho\left[S_\mu, S_\nu\right]\right), \tag{43}$$

where $C\left(S_\mu, S_\nu\right)$ is the covariance between the two spin operators.

By exploiting the analytical expressions for the correlation and the expectation values of the S_μ's for the XY model (see Refs. [92–94]), the compatibility index in Eq. (9) is readily evaluated. In Figure 6 is shown the behaviour of the quantumness R_φ for different sets of the Hamiltonian parameters and for different numbers of spins. In all the configurations the values of R_φ, close to zero in the ferromagnetic region, increase gradually for $\lambda < \lambda_C(=1)$. When the critical point $\lambda = \lambda_C$ is reached the quantumness abruptly saturate to its maximum value $R_\varphi = 1$. Hence, the system goes from maximal incompatibility in the paramagnetic phase to a relatively compatible situation in the ferromagnetic phase, with a more pronounced transition as the number of spins increases. Intuitively, the high compatibility in the ferromagnetic region can be ascribed to the multipartite entanglement of ρ_0. Indeed, the form of ρ_0 in the ferromagnetic phase bears close similarity to the density matrix of the GHZ states [49], which are optimal probes for multi-parameter quantum magnetometry [3].
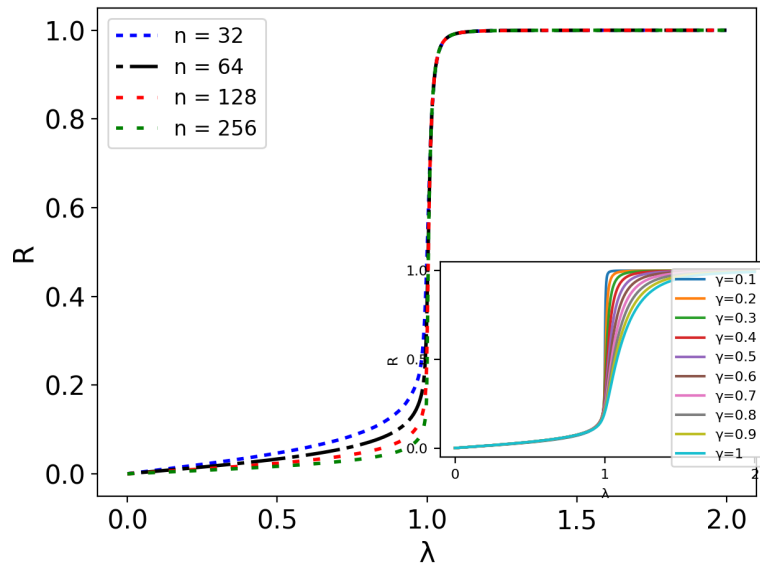
Figure 6: The compatibility index $R(n, \lambda)$ for the XY Ising chain at different values of n, up to $n = 256$, with $\gamma = 0.2$ as a function of λ. Inset: the compatibility index $R(\gamma, \lambda)$ for the XY Ising chain, for different values of $\gamma \in (0, 1]$ and $n = 64$, as a function of λ. The behaviour of R in the parametric regions appears to sharpen as γ gets closer to 0. This effect can be seen in the inset of Fig. 6, that displays the different behaviour of R as γ varies in $(0, 1]$, with n fixed.

References

[1] H. Cramér, *Mathematical methods of statistics*, Princeton University Press, ISBN 0691080046 (1946).

[2] C. W. Helstrom, *Quantum detection and estimation theory*, Academic Press, ISBN 0123400503 (1976).

[3] T. Baumgratz and A. Datta, *Quantum Enhanced Estimation of a Multidimensional Field*, Phys. Rev. Lett. **116**(3), 030801 (2016), doi:10.1103/PhysRevLett.116.030801.

[4] I. Apellaniz, I. Urizar-Lanz, Z. Zimborás, P. Hyllus and G. Tóth, *Precision bounds for gradient magnetometry with atomic ensembles*, Phys. Rev. A **97**(5), 053603 (2018), doi:10.1103/PhysRevA.97.053603.

[5] P. C. Humphreys, M. Barbieri, A. Datta and I. A. Walmsley, *Quantum Enhanced Multiple Phase Estimation*, Phys. Rev. Lett. **111**(7), 070403 (2013), doi:10.1103/PhysRevLett.111.070403.

[6] C. N. Gagatsos, D. Branford and A. Datta, *Gaussian systems for quantum-enhanced multiple phase estimation*, Phys. Rev. A **94**, 042342 (2016), doi:10.1103/PhysRevA.94.042342.

[7] M. Tsang, R. Nair and X.-M. Lu, *Quantum Theory of Superresolution for Two Incoherent Optical Point Sources*, Phys. Rev. X **6**(3), 031033 (2016), doi:10.1103/PhysRevX.6.031033.

[8] J. Řeháček, Z. Hradil, B. Stoklasa, M. Paúr, J. Grover, A. Krzic and L. L. Sánchez-Soto, *Multiparameter quantum metrology of incoherent point sources: Towards realistic superresolution*, Phys. Rev. A **96**, 062107 (2017), doi:10.1103/PhysRevA.96.062107.

[9] A. Chrostowski, R. Demkowicz-Dobrzański, M. Jarzyna and K. Banaszek, *On super-resolution imaging as a multiparameter estimation problem*, Int. J. Quantum Inf. **15**(8), 1 (2017), doi:10.1142/S0219749917400056.

[10] Z. Yu and S. Prasad, *Quantum Limited Superresolution of an Incoherent Source Pair in Three Dimensions*, Phys. Rev. Lett. **121**(18), 180504 (2018), doi:10.1103/PhysRevLett.121.180504.

[11] D. Braun, G. Adesso, F. Benatti, R. Floreanini, U. Marzolino, M. W. Mitchell and S. Pirandola, *Quantum-enhanced measurements without entanglement*, Rev. Mod. Phys. **90**(3), 035006 (2018), doi:10.1103/RevModPhys.90.035006.

[12] M. Szczykulska, T. Baumgratz and A. Datta, *Multi-parameter quantum metrology*, Adv. Phys. X **1**(4), 621 (2016), doi:10.1080/23746149.2016.1230476.

[13] F. Albarelli, M. Barbieri, M. Genoni and I. Gianani, *A perspective on multiparameter quantum metrology: From theoretical tools to applications in quantum imaging*, Phys. Lett. A **384**(12), 126311 (2020), doi:10.1016/j.physleta.2020.126311.

[14] L. Bakmou, A. Slaoui, M. Daoud and R. Ahl Laamara, *Quantum fisher information matrix in heisenberg xy model*, Quantum Information Processing **18**(6), 163 (2019), doi:10.1007/s11128-019-2282-x.

[15] G. M. D'Ariano and M. G. A. Paris, *Arbitrary precision in multipath interferometry*, Phys. Rev. A **55**, 2267 (1997), doi:10.1103/PhysRevA.55.2267.

[16] C. Macchiavello, *Optimal estimation of multiple phases*, Phys. Rev. A **67**, 062302 (2003), doi:10.1103/PhysRevA.67.062302.

[17] M. A. Ballester, *Entanglement is not very useful for estimating multiple phases*, Phys. Rev. A **70**, 032310 (2004), doi:10.1103/PhysRevA.70.032310.

[18] K. C. Young, M. Sarovar, R. Kosut and K. B. Whaley, *Optimal quantum multiparameter estimation and application to dipole- and exchange-coupled qubits*, Phys. Rev. A **79**, 062301 (2009), doi:10.1103/PhysRevA.79.062301.

[19] C. Vaneph, T. Tufarelli and M. G. Genoni, *Quantum estimation of a two-phase spin rotation*, Quantum Meas. Quantum Metrol. **1**(1), 12 (2013), doi:10.2478/qmetro-2013-0003.

[20] M. G. Genoni, M. G. A. Paris, G. Adesso, H. Nha, P. L. Knight and M. S. Kim, *Optimal estimation of joint parameters in phase space*, Phys. Rev. A **87**, 012107 (2013), doi:10.1103/PhysRevA.87.012107.

[21] Y.-R. Zhang and H. Fan, *Quantum metrological bounds for vector parameters*, Phys. Rev. A **90**, 043818 (2014), doi:10.1103/PhysRevA.90.043818.

[22] H. Yuan and C.-H. F. Fung, *Optimal feedback scheme and universal time scaling for hamiltonian parameter estimation*, Phys. Rev. Lett. **115**, 110401 (2015), doi:10.1103/PhysRevLett.115.110401.

[23] D. W. Berry, M. Tsang, M. J. W. Hall and H. M. Wiseman, *Quantum bell-ziv-zakai bounds and heisenberg limits for waveform estimation*, Phys. Rev. X **5**, 031018 (2015), doi:10.1103/PhysRevX.5.031018.

[24] N. Li, C. Ferrie, J. A. Gross, A. Kalev and C. M. Caves, *Fisher-Symmetric Informationally Complete Measurements for Pure States*, Phys. Rev. Lett. **116**(18), 180402 (2016), doi:10.1103/PhysRevLett.116.180402.

[25] J. Liu and H. Yuan, *Control-enhanced multiparameter quantum estimation*, Phys. Rev. A **96**, 042114 (2017), doi:10.1103/PhysRevA.96.042114.

[26] N. Liu and H. Cable, *Quantum-enhanced multi-parameter estimation for unitary photonic systems*, Quantum Sci. Technol. **2**(2) (2017), doi:10.1088/2058-9565/aa6fea.

[27] L. Pezzè, M. A. Ciampini, N. Spagnolo, P. C. Humphreys, A. Datta, I. A. Walmsley, M. Barbieri, F. Sciarrino and A. Smerzi, *Optimal Measurements for Simultaneous Quantum Estimation of Multiple Phases*, Phys. Rev. Lett. **119**(13), 130504 (2017), doi:10.1103/PhysRevLett.119.130504.

[28] H. Yuan and C.-H. F. Fung, *Quantum metrology matrix*, Phys. Rev. A **96**, 012310 (2017), doi:10.1103/PhysRevA.96.012310.

[29] Z. Eldredge, M. Foss-Feig, J. A. Gross, S. L. Rolston and A. V. Gorshkov, *Optimal and secure measurement protocols for quantum sensor networks*, Phys. Rev. A **97**, 042337 (2018), doi:10.1103/PhysRevA.97.042337.

[30] R. Nair, *Quantum-Limited Loss Sensing: Multiparameter Estimation and Bures Distance between Loss Channels*, Phys. Rev. Lett. **121**(23), 230801 (2018), doi:10.1103/PhysRevLett.121.230801.

[31] R. Nichols, P. Liuzzo-Scorpo, P. A. Knott and G. Adesso, *Multiparameter gaussian quantum metrology*, Phys. Rev. A **98**, 012114 (2018), doi:10.1103/PhysRevA.98.012114.

[32] M. Gessner, L. Pezzè and A. Smerzi, *Sensitivity bounds for multiparameter quantum metrology*, Phys. Rev. Lett. **121**, 130503 (2018), doi:10.1103/PhysRevLett.121.130503.

[33] N. Kura and M. Ueda, *Finite-error metrological bounds on multiparameter hamiltonian estimation*, Phys. Rev. A **97**, 012101 (2018), doi:10.1103/PhysRevA.97.012101.

[34] H. Chen and H. Yuan, *Optimal joint estimation of multiple rabi frequencies*, Phys. Rev. A **99**, 032122 (2019), doi:10.1103/PhysRevA.99.032122.

[35] H. Chen and H. Yuan, *Optimal joint estimation of multiple Rabi frequencies*, Phys. Rev. A **99**(3), 1 (2019), doi:10.1103/PhysRevA.99.032122.

[36] J. Rubio and J. Dunningham, *Bayesian multiparameter quantum metrology with limited data*, Phys. Rev. A **101**(3), 032114 (2020), doi:10.1103/PhysRevA.101.032114.

[37] A. Carollo, B. Spagnolo, A. A. Dubkov and D. Valenti, *On quantumness in multiparameter quantum estimation*, J. Stat. Mech. Theory Exp. **2019**(9), 094010 (2019), doi:10.1088/1742-5468/ab3ccb.

[38] S. Roy, *Fundamental noisy multiparameter quantum bounds*, Sci. Rep. **9**(1), 1038 (2019), doi:10.1038/s41598-018-37583-7.

[39] F. Albarelli, J. F. Friel and A. Datta, *Evaluating the Holevo Cramér-Rao Bound for Multiparameter Quantum Metrology*, Phys. Rev. Lett. **123**(20), 200503 (2019), doi:10.1103/PhysRevLett.123.200503.

[40] J. S. Sidhu, Y. Ouyang, E. T. Campbell and P. Kok, *Tight Bounds on the Simultaneous Estimation of Incompatible Parameters*, Phys. Rev. X **11**(1), 011028 (2021), doi:10.1103/PhysRevX.11.011028.

[41] M. Tsang, F. Albarelli and A. Datta, *Quantum Semiparametric Estimation*, Phys. Rev. X **10**(3), 031023 (2020), doi:10.1103/PhysRevX.10.031023.

[42] R. Demkowicz-Dobrzański, W. Górecki and M. Guţă, *Multi-parameter estimation beyond quantum Fisher information*, J. Phys. A Math. Theor. **53**(36), 363001 (2020), doi:10.1088/1751-8121/ab8ef3.

[43] E. Polino, M. Riva, M. Valeri, R. Silvestri, G. Corrielli, A. Crespi, N. Spagnolo, R. Osellame and F. Sciarrino, *Experimental multiphase estimation on a chip*, Optica **6**(3), 288 (2019), doi:10.1364/OPTICA.6.000288.

[44] M. Parniak, S. Borówka, K. Boroszko, W. Wasilewski, K. Banaszek and R. Demkowicz-Dobrzański, *Beating the Rayleigh Limit Using Two-Photon Interference*, Phys. Rev. Lett. **121**(25), 250503 (2018), doi:10.1103/PhysRevLett.121.250503.

[45] E. Roccia, V. Cimini, M. Sbroscia, I. Gianani, L. Ruggiero, L. Mancino, M. G. Genoni, M. A. Ricci and M. Barbieri, *Multiparameter approach to quantum phase estimation with limited visibility*, Optica **5**(10), 1171 (2018), doi:10.1364/OPTICA.5.001171.

[46] E. Roccia, I. Gianani, L. Mancino, M. Sbroscia, F. Somma, M. G. Genoni and M. Barbieri, *Entangling measurements for multiparameter estimation with two qubits*, Quantum Sci. Technol. **3**(1), 01LT01 (2018), doi:10.1088/2058-9565/aa9212.

[47] M. D. Vidrighin, G. Donati, M. G. Genoni, X. M. Jin, W. S. Kolthammer, M. S. Kim, A. Datta, M. Barbieri and I. A. Walmsley, *Joint estimation of phase and phase diffusion for quantum metrology*, Nat. Commun. **5**, 1 (2014), doi:10.1038/ncomms4532.

[48] G. Mussardo, S. Navigation and N. S. Route, *Statistical field theory : an introduction to exactly solved models in statistical physics*, Oxford University Press, ISBN 9780199547586 (2010).

[49] S. Sachdev, *Quantum Phase Transitions*, Cambridge University press, ISBN 9780521514682 (2011).

[50] P. Zanardi, M. G. A. Paris and L. Campos Venuti, *Quantum criticality as a resource for quantum estimation*, Phys. Rev. A **78**(4), 042105 (2008), doi:10.1103/PhysRevA.78.042105.

[51] C. Invernizzi, M. Korbman, L. Campos Venuti and M. G. A. Paris, *Optimal quantum estimation in spin systems at criticality*, Phys. Rev. A **78**, 042106 (2008), doi:10.1103/PhysRevA.78.042106.

[52] M. Tsang, *Quantum transition-edge detectors*, Phys. Rev. A **88**, 021801 (2013), doi:10.1103/PhysRevA.88.021801.

[53] P. A. Ivanov and D. Porras, *Adiabatic quantum metrology with strongly correlated quantum optical systems*, Phys. Rev. A **88**, 023803 (2013), doi:10.1103/PhysRevA.88.023803.

[54] M. Bina, I. Amelio and M. G. A. Paris, *Dicke coupling by feasible local measurements at the superradiant quantum phase transition*, Phys. Rev. E **93**(5), 052118 (2016), doi:10.1103/PhysRevE.93.052118.

[55] I. Frérot and T. Roscilde, *Quantum Critical Metrology*, Phys. Rev. Lett. **121**(2), 020402 (2018), doi:10.1103/PhysRevLett.121.020402.

[56] T. L. Heugel, M. Biondi, O. Zilberberg and R. Chitra, *Quantum transducer using a parametric driven-dissipative phase transition*, Phys. Rev. Lett. **123**(17), 173601 (2019), doi:10.1103/PhysRevLett.123.173601.

[57] L. Garbe, M. Bina, A. Keller, M. G. A. Paris and S. Felicetti, *Critical Quantum Metrology with a Finite-Component Quantum Phase Transition*, Phys. Rev. Lett. **124**(12), 120504 (2020), doi:10.1103/PhysRevLett.124.120504.

[58] P. A. Ivanov, *Steady-state force sensing with single trapped ion*, Phys. Scr. **95**(2), 025103 (2020), doi:10.1088/1402-4896/ab444c.

[59] V. Montenegro, U. Mishra and A. Bayat, *Global Sensing and Its Impact for Quantum Many-Body Probes with Criticality*, Phys. Rev. Lett. **126**(20), 200501 (2021), doi:10.1103/PhysRevLett.126.200501.

[60] H. Zhu, *Information complementarity: A new paradigm for decoding quantum incompatibility*, Sci. Rep. **5**, 1 (2015), doi:10.1038/srep14317.

[61] S. Ragy, M. Jarzyna and R. Demkowicz-Dobrzański, *Compatibility in multiparameter quantum metrology*, Phys. Rev. A **94**(5), 052108 (2016), doi:10.1103/PhysRevA.94.052108.

[62] Z. Hou, J. F. Tang, J. Shang, H. Zhu, J. Li, Y. Yuan, K. D. Wu, G. Y. Xiang, C. F. Li and G. C. Guo, *Deterministic realization of collective measurements via photonic quantum walks*, Nat. Commun. **9**(1), 1 (2018), doi:10.1038/s41467-018-03849-x.

[63] A. Carollo, B. Spagnolo, A. A. Dubkov and D. Valenti, *Erratum: On quantumness in multiparameter quantum estimation (2019 J. Stat. Mech . 094010)*, J. Stat. Mech. Theory Exp. **2020**(2), 029902 (2020), doi:10.1088/1742-5468/ab6f5e.

[64] A. Holevo, *Probabilistic and Statistical Aspects of Quantum Theory*, Edizioni della Normale, Pisa, ISBN 978-88-7642-375-8, doi:10.1007/978-88-7642-378-9 (2011).

[65] S. L. Braunstein and C. M. Caves, *Statistical distance and the geometry of quantum states*, Phys. Rev. Lett. **72**(22), 3439 (1994), doi:10.1103/PhysRevLett.72.3439.

[66] M. Guţă and J. Kahn, *Local asymptotic normality for qubit states*, Phys. Rev. A **73**, 052108 (2006), doi:10.1103/PhysRevA.73.052108.

[67] M. Hayashi and K. Matsumoto, *Asymptotic performance of optimal state estimation in qubit system*, J. Math. Phys. **49**(10), 102101 (2008), doi:10.1063/1.2988130.

[68] J. Kahn and M. Gu\c{t}\u{a}, *Local Asymptotic Normality for Finite Dimensional Quantum Systems*, Commun. Math. Phys. **289**(2), 597 (2009), doi:10.1007/s00220-009-0787-3.

[69] K. Yamagata, A. Fujiwara and R. D. Gill, *Quantum local asymptotic normality based on a new quantum likelihood ratio*, Ann. Stat. **41**(4), 2197 (2013), doi:10.1214/13-AOS1147.

[70] F. Yang, V. Perrin, A. Petrescu, I. Garate and K. Le Hur, *From topological superconductivity to quantum Hall states in coupled wires*, Phys. Rev. B **101**(8), 085116 (2020), doi:10.1103/PhysRevB.101.085116.

[71] J. Suzuki, *Explicit formula for the Holevo bound for two-parameter qubit-state estimation problem*, J. Math. Phys. **57**(4), 042201 (2016), doi:10.1063/1.4945086.

[72] K. Matsumoto, *A new approach to the Cramer – Rao-type bound of the pure-state model*, J. Phys. A. Math. Gen. **35**, 3111 (2002).

[73] M. Bradshaw, S. M. Assad and P. K. Lam, *A tight Cramér–Rao bound for joint parameter estimation with a pure two-mode squeezed probe*, Phys. Lett. Sect. A Gen. At. Solid State Phys. **381**(32), 2598 (2017), doi:10.1016/j.physleta.2017.06.024.

[74] M. Bradshaw, P. K. Lam and S. M. Assad, *Ultimate precision of joint quadrature parameter estimation with a gaussian probe*, Phys. Rev. A **97**, 012106 (2018), doi:10.1103/PhysRevA.97.012106.

[75] A. Carollo, B. Spagnolo and D. Valenti, *Uhlmann curvature in dissipative phase transitions*, Sci. Rep. **8**(1), 9852 (2018), doi:10.1038/s41598-018-27362-9.

[76] A. Candeloro, M. G. A. Paris and M. G. Genoni, *On the properties of the asymptotic incompatibility measure in multiparameter quantum estimation* (2021), 2107.13426.

[77] S. Razavian, M. G. A. Paris and M. G. Genoni, *On the Quantumness of Multi-parameter Estimation Problems for Qubit Systems*, Entropy **22**(11), 1197 (2020), doi:10.3390/e22111197.

[78] A. Carollo, D. Valenti and B. Spagnolo, *Geometry of quantum phase transitions*, Phys. Rep. **838**, 1 (2020), doi:10.1016/j.physrep.2019.11.002.

[79] D. Rossini and E. Vicari, *Ground-state fidelity at first-order quantum transitions*, Phys. Rev. E **98**(6), 062137 (2018), doi:10.1103/PhysRevE.98.062137.

[80] M. Campostrini, J. Nespolo, A. Pelissetto and E. Vicari, *Finite-size scaling at first-order quantum transitions*, Phys. Rev. Lett. **113**, 070402 (2014), doi:10.1103/PhysRevLett.113.070402.

[81] L. Campos Venuti and P. Zanardi, *Quantum Critical Scaling of the Geometric Tensors*, Phys. Rev. Lett. **99**(9), 095701 (2007), doi:10.1103/PhysRevLett.99.095701.

[82] L. Leonforte, D. Valenti, B. Spagnolo and A. Carollo, *Uhlmann number in translational invariant systems*, Sci. Rep. **9**(1), 9106 (2019), doi:10.1038/s41598-019-45546-9.

[83] H. P. Robertson, *The Uncertainty Principle*, Phys. Rev. **34**(1), 163 (1929), doi:10.1103/PhysRev.34.163.

[84] R. Demkowicz-Dobrzański, M. Jarzyna and J. Kołodyński, *Chapter Four - Quantum Limits in Optical Interferometry*, vol. 60 of *Progress in Optics*, pp. 345–435. Elsevier, doi:https://doi.org/10.1016/bs.po.2015.02.003 (2015).

[85] S.-J. Gu, *Fidelity Approach to Quantum Phase Transitions*, Int. J. Mod. Phys. B **24**(23), 4371 (2010), doi:10.1142/S0217979210056335.

[86] M. E. Reuter, M. J. Hartmann and M. B. Plenio, *Geometric phases and critical phenomena in a chain of interacting spins*, Proc. R. Soc. A Math. Phys. Eng. Sci. **463**(2081), 1271 (2007), doi:10.1098/rspa.2007.1822.

[87] V. Bargmann, *Note On {W}igners Theorem On Symmetry Operations*, J. Math. Phys. **5**, 862 (1964).

[88] N. Mukunda and R. Simon, *Quantum Kinematic Approach to the Geometric Phase. I. General Formalism*, Ann. Phys. (N. Y). **228**(2), 205 (1993), doi:10.1006/aphy.1993.1093.

[89] O. F. d. A. Bonfim, B. Boechat and J. Florencio, *Ground-state properties of the one-dimensional transverse ising model in a longitudinal magnetic field*, Phys. Rev. E **99**, 012122 (2019), doi:10.1103/PhysRevE.99.012122.

[90] A. A. Ovchinnikov, D. V. Dmitriev, V. Y. Krivnov and V. O. Cheranovskii, *Antiferromagnetic ising chain in a mixed transverse and longitudinal magnetic field*, Phys. Rev. B **68**, 214406 (2003), doi:10.1103/PhysRevB.68.214406.

[91] A. Uhlmann, *The "transition probability" in the state space of a *-algebra*, Reports Math. Phys. **9**(2), 273 (1976), doi:10.1016/0034-4877(76)90060-4.

[92] W. F. Liu, J. Ma and X. Wang, *Quantum Fisher information and spin squeezing in the ground state of the XY model*, J. Phys. A Math. Theor. **46**(4) (2013), doi:10.1088/1751-8113/46/4/045302.

[93] E. H. Lieb, T. Schultz and D. Mattis, *Two soluble models of an antiferromagnetic chain*, Ann. Phys. (N. Y). **16**(3), 407 (1961), doi:10.1016/0003-4916(61)90115-4.

[94] E. Barouch and B. M. McCoy, *Statistical mechanics of the XY model. II. Spin-correlation functions*, Phys. Rev. A **3**(2), 786 (1971), doi:10.1103/PhysRevA.3.786.